References

[1] Pappis, J., "The mechanical properties of pyrolytic graphite," *Mechanical Properties of Engineering Ceramics*, edited by W. Kriegel and H. Palmour III (Interscience Publishers, Inc., New York, 1960), Chap. 25, pp. 429–450.

[2] Lozier, W. W. and Manofsky, M. B., "Properties and performance of pyrolytic graphite," *Mechanical Properties of Engineering Ceramics*, edited by W. Kriegel and H. Palmour III (Interscience Publishers, Inc., New York, 1960), Chap. 26, pp. 351–473.

[3] Diefendorf, R. J. and Stover, E. R., "Pyrolytic graphite—how structure affects properties," Metals Progr. **81**, 103–108 (1962).

[4] Schiff, D., "Pyrolytic materials for re-entry applications," Metals Engineering Quarterly **2**, 32–42 (1962).

[5] Riley, M. W., "The new world of graphite," Mater. Design Eng. **56**, 113–128 (1962).

[6] Pappis, J. and Blum, S., "Properties of pyrolytic graphite," J. Am. Ceram. Soc. **44**, 592–597 (1961).

[7] "Pyrolytic graphite data book," Lockheed Missile and Space Div. LMSD 288186 (April 14, 1961).

[8] Smith, W. H., "Mechanical properties of pyrolytic graphite—2. Effect of structure on strength at room temperature," General Electric Co. Memo. MF109, Part F (May 1960).

[9] Berry, J. M. and Gebhardt, J. J., "Interpretation of room temperature mechanical properties tests on pyrolytic graphite," J. Am. Ceram. Soc. (to be published).

[10] *The Industrial Graphite Engineering Handbook*, (Carbon Products Division, Union Carbide Corp., New York, Revised April 1964).

[11] Stover, E. R., "Flame polishing pyrolytic graphite," Metals Progr. **83**, 112–113 (1963).

FEBRUARY 1965 AIAA JOURNAL VOL. 3, NO. 2

Influence of Cushion Stiffness on the Stability of Cushion-Loaded Cylindrical Shells

D. O. BRUSH*
University of California, Davis, Calif.

AND

E. V. PITTNER†
Lockheed Missiles and Space Company, Palo Alto, Calif.

This paper presents results of a theoretical analysis of the influence of cushion stiffness on the buckling strength of cylindrical shells subjected to soft elastic cushion pressure. A stability equation is derived for a simply supported cylinder subjected to an axisymmetric band of cushion pressure applied at an arbitrary distance from one end of the cylinder. An exact solution is given for the limiting case of a circular ring or infinitely long cylinder under uniform elastic cushion pressure. For the more general case of a finite-length cylinder with an arbitrarily located band of cushions, infinite series are utilized in the solution. Extensive numerical results are presented in graphical form. They indicate that buckling pressures in general are much higher under cushion loading than under fluid-pressure loading. They also indicate that cylinder length and cushion location are unimportant unless the cylinder is rather short or the cushion is near one end. In such cases, however, the stabilizing influence of end rings is quite strong. Results are in agreement with previously available theoretical results for various limiting cases and with limited available test data.

Nomenclature

D	=	bending stiffness
E	=	Young's modulus
J_3	=	Eq. (8)
$K_m{}^n$	=	Eq. (9)
K_s	=	cushion stiffness coefficient, Eq. (A4)
L	=	length of cylindrical shell
V	=	total potential energy
W_s	=	work of cushion pressure
a	=	middle-surface radius
b	=	cushion width
c	=	distance from center of cushion to near end of cylinder
h	=	shell thickness
h_s	=	cushion thickness at impending buckling
k, m, n	=	wavelength parameters, Eq. (3)
p	=	pressure applied to cylinder by cushion
p_{cr}	=	buckling pressure
q	=	number of circumferential waves in buckled form
v, w	=	nondimensional tangential and radial displacement components of a point on the shell's middle surface; the corresponding distances are av, aw, and w is positive inward
α	=	L/a
ν	=	Poisson's ratio
η_m, ψ_k, J_1	=	Eq. (3)
λ	=	cushion thickness parameter, Eq. (A4)

Subscripts

0	=	prebuckling quantities
1	=	incremental quantities
s	=	cushion

Received May 1, 1964; revision received August 28, 1964.

* Professor of Engineering; formerly Senior Staff Scientist, Research Laboratories, Lockheed Missiles and Space Company, Palo Alto, Calif. Member AIAA.

† Research Specialist, Research Laboratories. Member AIAA.

Introduction

RADIAL pressure applied to the lateral surface of a rocket motor case by soft elastic cushions induces compressive hoop stresses in the motor case skin. If the cushions are suf-

ficiently soft, these hoop stresses can cause the shell to fail by buckling. In such cases, the stiffness of the cushioning material is a major factor in determining the magnitude of the applied pressure at which buckling occurs. The cushions furnish a stabilizing restraint that is similar to that derived from the propellant in a solid-rocket motor case. Softer cushions result in lower buckling pressures, and the limiting case of zero cushion stiffness corresponds to ordinary fluid-pressure loading.

This paper presents results of a theoretical analysis of the influence of cushion stiffness on the buckling strength of cylindrical shells subjected to soft elastic cushion pressure. A stability equation is given for a simply supported cylinder subjected to an axisymmetric band of cushion pressure applied at an arbitrary distance from one end of the cylinder. The equation is obtained by extending an earlier analysis for fluid-pressure loading[1] to take into account the influence of the loading cushion stiffness. The cushion is treated as a linearly elastic foundation. For simplicity it is also assumed to act as a plane stress medium during buckling; shear coupling is taken into account in the circumferential direction but is neglected in the axial direction. The simplification is based on the observation that, as indicated in tests of cylindrical shells subjected to a circumferential band of fluid pressure,[2] buckling displacements within the region of the pressure band are almost uniform in the axial direction, but highly nonuniform in the circumferential direction. The assumption has negligible influence for thin cushions for which all shear coupling may be neglected and is moderately conservative for thicker cushions.

The object of the stability analysis is to determine the critical value of the pressure between cushion and cylinder at which the cylinder buckles. Prior to buckling, uniform pressure is applied to the outer surface of the cushion (Fig. 1), and increased at an infinitesimal rate. The cushion and shell are compressed but remain axisymmetric. The axisymmetric form is an equilibrium configuration for any value of applied pressure, but for sufficiently high pressures the form is unstable. The buckling pressure is defined as the limiting value of the pressure between cushion and cylinder at which the axisymmetric form loses its stability. The stability criterion is based on the minimum potential energy theory of stability. At a certain level of applied pressure, the outer perimeter of the cushion is held fixed, and the shell is given a small virtual incremental displacement. The system composed of the cushion and shell is necessarily conservative during the virtual deformation, if the interface surfaces are frictionless. The deformation is accompanied by a corresponding change in the total potential energy of the system. The axisymmetric equilibrium form is stable if the second variation of the total potential energy is positive-definite. The buckling pressure thus corresponds to the limiting pressure at which the second variation ceases to be positive-definite.

Analysis

Cylinder

Details of the analysis in Ref. 1 will not be repeated here. It may be noted that the cylinder analysis is based on a first-approximation or uncoupled strain energy expression and that the kinematic relations are identical to corresponding relations from Ref. 3 for the class of deformations characterized by small strains, "moderately-small" rotations about the coordinate lines, and negligibly small rotations about the normal. For the limiting case of uniform fluid pressure applied to the entire lateral surface of the cylinder, results of the analysis in Ref. 1 are in close numerical agreement with corresponding results based on the well-known Flügge equations for such loading.

To extend the analysis of Ref. 1 to take into account the influence of loading cushion stiffness, it is necessary only to replace the term representing the potential energy of the applied fluid pressure in the stability equation of Ref. 1 by a corresponding term representing the potential energy of the cushion pressure. The analysis in Ref. 1 leads to a linear eigenvalue problem, and the final stability equation is given in the form of a determinant of order M

$$\det K_m{}^n = 0 \qquad m, n = 1, 2, 3, \ldots, M \tag{1}$$

Equation (14) of Ref. 1 gives the following expression for $K_m{}^n$ for a cylindrical shell subjected to an axisymmetric band of fluid pressure applied at an arbitrary distance from one end of the cylinder:

$$K_m{}^n = A_m{}^n + B_m{}^n + C_m{}^n - \frac{2(1-\nu^2)}{\pi}\frac{p_0 a}{Eh}\left[D_m{}^n + E_m{}^n\right] \tag{2}$$

The terms $A_m{}^n$, $B_m{}^n$, and $D_m{}^n$ represent cylinder strain energy, including the so-called work of the membrane forces during buckling. The term $C_m{}^n$ represents the strain energy of a soft elastic core within the cylinder. In the interest of brevity, numerical results are presented here only for the case $C_m{}^n = 0$, i.e., for the empty cylinder. The term $E_m{}^n$ represents the potential energy of the applied fluid pressure. From Ref. 1,

$$\left.\begin{aligned}
A_m{}^n &= \delta_m{}^n\left[\left(\frac{m\pi}{\alpha}\right)^2\xi_m{}^2 + (q\eta_m - 1)^2 - 2\nu\frac{m\pi}{\alpha}\xi_m(q\eta_m - 1) + \frac{1-\nu}{2}\left(\frac{m\pi}{\alpha}\eta_m - q\xi_m\right)^2\right]\\
B_m{}^n &= \frac{\delta_m{}^n}{12}\left(\frac{h}{a}\right)^2\left[\left(\frac{m\pi}{\alpha}\right)^4 + q^2(q-\eta_m)^2 + 2\nu\left(\frac{m\pi}{\alpha}\right)^2 q(q-\eta_m) + 2(1-\nu)\left(\frac{m\pi}{\alpha}\right)^2(q-\eta_m/2)^2\right]\\
D_m{}^n &= (q-\eta_m)(q-\eta_n)\sum_{k=1,2,3}^{K}\left[\frac{\psi_k J_1(k,m,n)}{\mu_k}\right]
\end{aligned}\right\} \tag{3}$$

where

$$\delta_m{}^n = \begin{cases} 1 & m = n \\ 0 & m \neq n \end{cases}$$

$$\xi_m = \left(\frac{m\pi}{\alpha}\right)\left[q^2 - \nu\left(\frac{m\pi}{\alpha}\right)^2\right]\left[\left(\frac{m\pi}{\alpha}\right)^2 + q^2\right]^{-2}$$

$$\eta_m = q\left[(2+\nu)\left(\frac{m\pi}{\alpha}\right)^2 + q^2\right]\left[\left(\frac{m\pi}{\alpha}\right)^2 + q^2\right]^{-2}$$

$$\psi_k = \frac{2}{k\pi}\left[\cos\left(\frac{k\pi}{\alpha}\frac{c-b/2}{a}\right) - \cos\left(\frac{k\pi}{\alpha}\frac{c+b/2}{a}\right)\right]$$

$$\mu_k = 1 + \frac{(h/a)^2}{12(1-\nu^2)}\left(\frac{k\pi}{\alpha}\right)^4$$

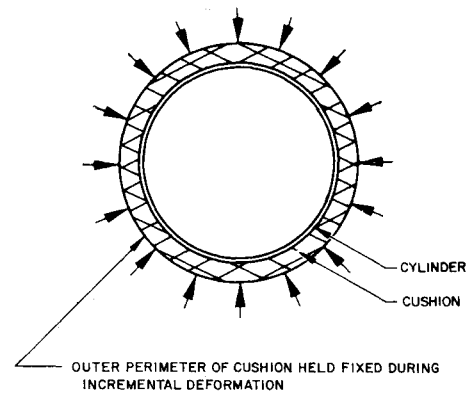

Fig. 1 Cross section of cylinder and cushion.

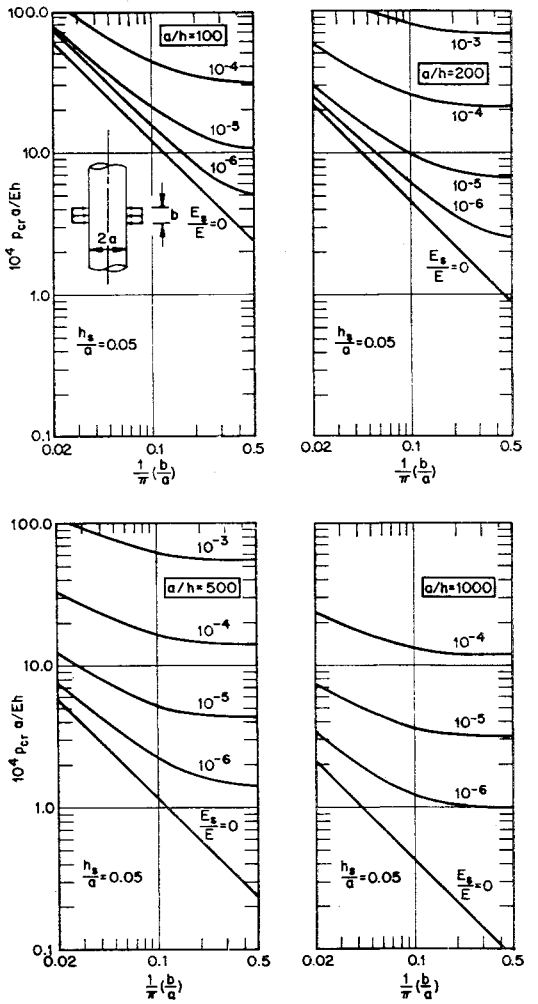

Fig. 2 Critical cushion pressures, infinitely long cylinders.

$$J_1(k, m, n) = \begin{cases} \dfrac{-4kmn}{(k^4 + m^4 + n^4) - 2[(km)^2 + (mn)^2 + (nk)^2]} \\ \quad \text{for } (k + m + n) = 1, 3, 5, \ldots \\ 0 \quad \text{for } (k + m + n) = 2, 4, 6, \ldots \end{cases}$$

and q, the number of circumferential waves in the buckled form, is an integer greater than unity.

In the formulation of an expression for the potential energy of the cushion pressure, the cylinder and cushion are assumed to remain in contact at all points during the virtual deformation, and the contact surfaces are assumed to be smooth. At impending buckling, the load dP applied by the cushion to an element of the shell surface is equal to $p_0a^2dxd\varphi$ and is radially directed. During the virtual deformation, the surface element undergoes an infinitesimal displacement (au_1, av_1, aw_1) and rotates through small angles ω_{x1}, $\omega_{\varphi 1}$, and its area changes from $a^2dxd\varphi$ to $(1 + \epsilon_{x1})(1 + \epsilon_{\varphi 1})\, a^2dxd\varphi$. The magnitude of the cushion pressure also changes an infinitesimal amount to $(p_0 + p_1)$. The small contributions of $\omega_{\varphi 1}$ and ϵ_{x1} neglected, the radial and tangential components of the load dP after the virtual deformation therefore are approximately $[p_0 + p_0(\partial v_1/\partial\varphi - w_1) + p_1]a^2dxd\varphi$ and $p_0(v_1 + \partial w_1/\partial\varphi)a^2dxd\varphi$, respectively. An additional axial component is small and is neglected. The work of the load dP during the virtual deformation is then approximately

$$W_s = a^3 \int_0^{2\pi} \int_{[(c-b/2)/a]}^{[(c+b/2)/a]} \left[p_0 w_1 + \frac{1}{2} p_0 \left(\frac{\partial v_1}{\partial \varphi} - w_1 \right) w_1 + \frac{1}{2} p_1 w_1 - \frac{1}{2} p_0 \left(v_1 + \frac{\partial w_1}{\partial \varphi} \right) v_1 \right] dx d\varphi \quad (4)$$

where x and φ are nondimensional axial and circumferential coordinates.

The second variation of W_s is the sum of the second-order terms in the incremental quantities in Eq. (4), and may be written

$$\begin{aligned} \tfrac{1}{2}\,\delta^2 W_s &= \tfrac{1}{2}\,(\delta^2 W_s' + \delta^2 W_s'') \\ \delta^2 W_s' &= a^3 \int_0^{2\pi} \int_{[(c-b/2)/a]}^{[(c+b/2)/a]} [p_1 w_1]\, dx d\varphi \\ \delta^2 W_s'' &= a^3 \int_0^{2\pi} \int_{[(c-b/2)/a]}^{[(c+b/2)/a]} \left[p_0 \left(w_1^2 - \frac{\partial v_1}{\partial \varphi} w_1 + v_1 \frac{\partial w_1}{\partial \varphi} + v_1^2 \right) \right] dx d\varphi \end{aligned} \quad (5)$$

where, from Eq. (A3), $p_1 = -K_s E_s w_1$.

With a change in sign, the p_1 term in Eq. (5) may be identified as the second variation of the potential energy of a constant-direction elastic pressure p_1, and the p_0 term as the corresponding quantity for a constant-magnitude fluid pressure p_0 (cf. Ref. 4). The influence of the p_0 term is negligibly small in almost all cases. Its influence is greatest (25% of the final result) in the limiting case of a ring or infinitely long cylinder under uniform fluid-pressure loading. The influence diminishes rapidly as the number of circumferential waves in the buckle pattern becomes larger than the classical ring value, $q = 2$.

The contribution of the cushion potential energy to the stability equation [Eq. (1)] accordingly may be written as the sum of two terms, $E_m{}^n$ and $G_m{}^n$, where $E_m{}^n$ represents the contribution of the constant-magnitude fluid pressure p_0 and is identical to the corresponding quantity in Ref. 1, and $G_m{}^n$ represents the contribution of the elastic pressure p_1. From Eq. (14) of Ref. 1,

$$E_m{}^n = [q(\eta_m + \eta_n) - 1 - \eta_m\eta_n] \sum_{k=1,2,3}^{K} [\psi_k J_1(k, m, n)] \quad (6)$$

By following the procedure of Ref. 1, and utilizing the displacement function

$$w_1 = \cos q\varphi \sum_{m=1,2}^{M} A_m \sin\frac{m\pi x}{\alpha}$$

the corresponding expression for $G_m{}^n$ is found to be

$$G_m{}^n = \frac{2(1 - \nu^2)}{\alpha} \frac{E_s a}{Eh} J_3(m, n) K_s \quad (7)$$

where

$$J_3(m, n) = \begin{cases} \dfrac{1}{2}\dfrac{b}{a} - \dfrac{\alpha}{2m\pi} \sin\left(\dfrac{m\pi}{\alpha}\dfrac{b}{a}\right) \cos\left(\dfrac{m\pi}{\alpha}\dfrac{2c}{a}\right) & m = n \\ \dfrac{\alpha}{\pi}\left[\dfrac{\sin\dfrac{(m-n)\pi b/a}{2\alpha} \cos\dfrac{(m-n)\pi c/a}{\alpha}}{m - n} - \dfrac{\sin\dfrac{(m+n)\pi b/a}{2\alpha} \cos\dfrac{(m+n)\pi c/a}{\alpha}}{m + n} \right] & m \neq n \end{cases} \quad (8)$$

and the cushion stiffness coefficient K_s is given by Eq. (A4). For cushion loading of a core-filled cylinder, accordingly, the right side of Eq. (2) must be augmented by the term $G_m{}^n$. For an empty cylinder $C_m{}^n = 0$, and Eq. (2) is replaced by the expression

$$K_m{}^n = A_m{}^n + B_m{}^n + G_m{}^n - \frac{2(1 - \nu^2)}{\pi} \frac{p_0 a}{Eh} [D_m{}^n + E_m{}^n] \quad (9)$$

The buckling pressure is thus given as the smallest eigenvalue p_0 of a determinant of order M. The value of M is chosen by trial to give the desired accuracy in the final result. The limit K on the summation of the prebuckling parameters in Eq. (2) is similarly chosen. For each q, we have one lowest eigenvalue, p_0. The smallest of all the p_0's represents the solution to the problem.

Ring

The circular ring is of special interest in the present investigation because it represents a limiting case of great practical importance and because it readily leads to an exact solution. Subtraction of the expression in Eq. (5) from the expression in Eq. (1) of Ref. 1 for the second variation of the strain energy of the cylinder, and specialization for a ring or uniformly loaded, infinitely long cylinder, gives the following equation for the second variation of the total potential energy of the system:

$$\delta^2 V = Ehab \int_0^{2\pi} [(v_1' - w_1)^2 - w_0(v_1 + w_1')^2 + \bar{D}(v_1' + w_1'')^2 - \frac{a}{Eh} p_1 w_1 + \frac{p_0 a}{Eh} (w_1^2 - v_1' w_1 + v_1 w_1' + v_1^2)]\, d\varphi \quad (10)$$

where

$$\bar{D} = D/(Eha^2) \text{ and } (\ )' = d(\ )/d\varphi$$

The critical pressure is the limiting value of p_0 at which the second variation expression ceases to be positive-definite. According to the Trefftz criterion, the limit of positive-definiteness of the second-variation expression is determined by the Euler equations for the integral.[5] From Eq. (10), these equations are

$$\begin{aligned} &(v_1' - w_1)' + \bar{D}(v_1 + w_1')'' + w_0(v_1 + w_1') - \frac{p_0 a}{Eh}(v_1 + w_1') = 0 \\ &-(v_1' - w_1) + \bar{D}(v_1 + w_1')''' + w_0(v_1 + w_1')' - \frac{p_0 a}{Eh}(v_1' - w_1) - \frac{p_1 a}{Eh} = 0 \end{aligned} \quad (11)$$

The required periodicity conditions are satisfied by the expressions

$$\begin{aligned} v_1 &= A_q \sin q\varphi \\ w_1 &= B_q \cos q\varphi \\ p_1/E_s &= C_q \cos q\varphi \end{aligned} \quad (12)$$

where, as before, q is an integer greater than unity. Introduction of these expressions into Eqs. (11) yields the equations

$$\left.\begin{aligned} &-q(qA_q - B_q) - \bar{D}q^2(A_q - qB_q) + w_0(A_q - qB_q) - (p_0 a/Eh)(A_q - qB_q) = 0 \\ &-(qA_q - B_q) - \bar{D}q^3(A_q - qB_q) + w_0 q(A_q - aB_q) - (p_0 a/Eh)(qA_q - B_q) - (E_s a/Eh)C_q = 0 \end{aligned}\right\} \quad (13)$$

But, from Eqs. (12) and (A3), $C_q = -K_s B_q$. Furthermore, for a thin ring, $p_0 a/Eh = w_0$. Therefore Eq. (13) can be written in the form

$$\begin{aligned} &q^2(1 + \bar{D})A_q - q(1 + q^2\bar{D})B_q = 0 \\ &-q(1 + q^2\bar{D})A_q + [(1 + q^4\bar{D} + K_s E_s a/Eh) - (q^2 - 1)(p_0 a/Eh)]B_q = 0 \end{aligned} \quad (14)$$

Equations (14) have a nontrivial solution only for particular values of the parameter $p_0 a/Eh$. By setting the determinant of the coefficients of A_q, B_q equal to zero, these are found to be

$$\frac{p_0 a}{Eh} = \frac{(q^2 - 1)\bar{D}}{1 + \bar{D}} + \frac{K_s E_s a/Eh}{q^2 - 1} \quad (15)$$

But $\bar{D} \ll 1$. Therefore

$$p_0 = (q^2 - 1)\frac{D}{a^3} + \frac{K_s E_s}{q^2 - 1} \quad (16)$$

Equation (16) represents the final solution for a ring or uniformly loaded, infinitely long cylinder. The value of q is determined by trial in the usual manner to yield the minimum critical pressure.

For fluid-pressure loading $E_s = 0$, and Eq. (16) reduces to the expression

$$p_0 = (q^2 - 1)(D/a^3) \quad (17)$$

Since q is an integer greater than unity, the critical pressure corresponds to $q = 2$, and

$$p_{cr} = 3\, D/a^3 \quad (18)$$

Equation (18) is the classical solution for this case.

Results

Cylinders

Numerical results based on the preceding equations are presented in graphical form. In all calculations, Poisson's ratio for the cylinder material was taken to be 0.3. Except where noted, Poisson's ratio for the cushion material was taken to be 0.5. In the interest of economy, most results shown are for values of the cushion thickness parameter $h_s/a = 0.05$.

Under cushion loading, the length of the cylinder is found to be an unimportant factor in determining critical pressure unless the cylinder is rather short. Accordingly, buckling pressures for "long" cylinders loaded at midlength are shown in Fig. 2. These results are based on Eqs. (1) and (9). For purposes of carrying out the calculations, the cylinder length was selected by trial to be too great to influence the results. Similar curves for long cylinders with the pressure band located adjacent to an end ring are given in Fig. 3. A corresponding set of curves for cylinders of moderate length subjected to uniform cushion pressure over their entire length, i.e., $b = L$, is shown in Fig. 4.

Selected results specifically illustrating the influence of cylinder length are presented in Fig. 5. Two cases are illustrated in each graph, one in which the pressure band is located at midlength, and the other in which the band is adjacent to an end ring. Figure 6 presents selected results to illustrate the influence of pressure band location. It may be seen that pressure band location is unimportant unless the band is near an end ring.

Rings

All of the cylindrical shell stability curves in Figs. 2–4 approach horizontal asymptotes for large values of the cushion width parameter b/a. These values may be determined from Eq. (16) for the infinitely long, uniformly loaded cylinder by letting the bending stiffness $D = Eh^3/[12(1 - \nu^2)]$. With this expression for D, Eq. (16) can be written in the nondimensional form

$$\frac{p_0 a}{Eh} = (q^2 - 1)\frac{(h/a)^2}{12(1 - \nu^2)} + \frac{K_s(E_s/E)(a/h)}{q^2 - 1} \quad (19)$$

where the stiffness coefficient K_s is given by Eq. (A4) or Fig. 7. Selected numerical results based on Eq. (19) are shown in Fig. 8 to illustrate the influence of cushion thickness. The curves show that the stabilizing influence of cushions is in-

versely related to their thickness. For sufficiently thin cushions, the stabilization is so great that buckling in the mode considered in this analysis is prevented entirely. However, at higher pressures, a snap-through mode of failure possibly can occur (cf. Ref. 6).

Because of the large number of design parameters for the cylindrical shell, it is convenient in practical applications to use Eq. (19) to establish a conservative first estimate of the buckling pressure. The curves in Figs. 2–4 may then be used to estimate any additional stabilizing influence of unloaded portions of the cylinder or of end rings.

Transverse Loading

Any circumferential distribution of applied pressure can be represented in terms of a cosine series:

$$p(\varphi) = p_0 + p_1 \cos\varphi + p_2 \cos 2\varphi + \ldots \qquad (20)$$

In such a representation, only the first harmonic $p_1 \cos\varphi$ is transverse; all of the others are self equilibrating. An analysis of cylindrical shell stability under a band of fluid pressure of the form

$$p = p_0 + p_1 \cos\varphi \qquad (21)$$

(where the subscripts, of course, refer to the number of the harmonic and not to prebuckling and incremental quantities) was presented by Almroth.[7] Results of that analysis indicate that the maximum allowable fluid pressure for such transverse loading is somewhat higher than for the corresponding axisymmetric loading. Furthermore the increase in most cases is small. Therefore, for design applications, the present critical values for axisymmetric cushion pressure probably furnish moderately conservative estimates of the corresponding values for transverse loadings of the form of Eq. (21).

The applied pressure distributions represented by Eq. (21) cause the cylinder cross sections to translate and diminish in diameter but (for the initially perfect shell) do not distort their circularity prior to buckling. However, the higher, self-equilibrating harmonics of loading in Eq. (20) ($p_2 \cos 2\varphi$, etc.) induce circumferential bending of the shell wall from the outset. Under such pressure distributions, the shell wall fails by nonlinear circumferential bending, i.e., local beam-column action, rather than by bifurcation instability. Therefore, for applied pressure distributions containing higher harmonics than those in Eq. (21), the present bifurcation analysis furnishes only an upper bound on the magnitude of the maximum allowable pressure. If the bending due to the higher, self-equilibrating harmonics is sufficiently limited, the bound is a close one. Of course, the nonlinear circumferential bending that is an inevitable consequence of shell shape imperfections and loading irregularities even under nominally axisymmetric loading also must be sufficiently limited.

Comparison with Existing Test Data

No entirely satisfactory test data appear to be available for a comparison of theoretical and experimental buckling pressures. The data shown in Fig. 9 were obtained from tests of full-sized simulated rocket motor cases reported by Miknis.[8] Two motor cases were used for the four test points shown. Each motor case was subjected to a transverse load

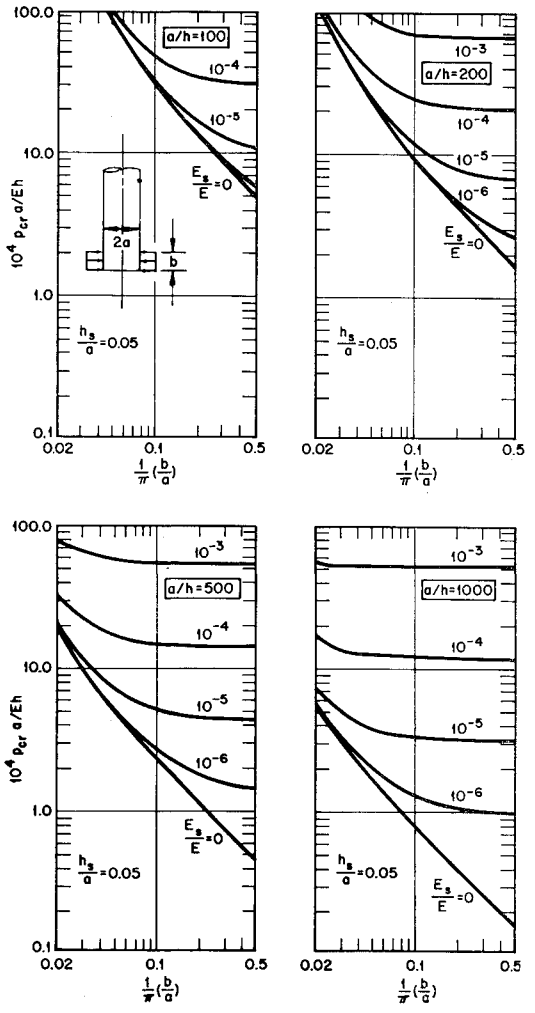

Fig. 3 Critical cushion pressures, semi-infinite cylinders.

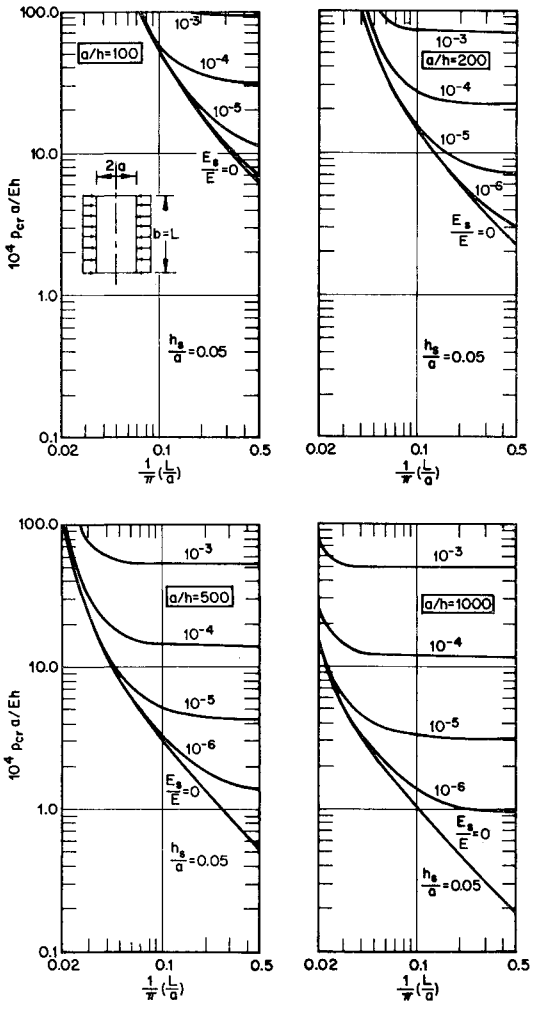

Fig. 4 Critical cushion pressures, uniform over-all pressure.

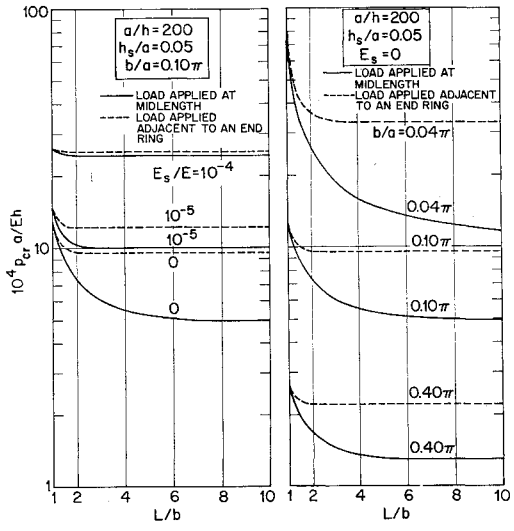

Fig. 5 Influence of cylinder length.

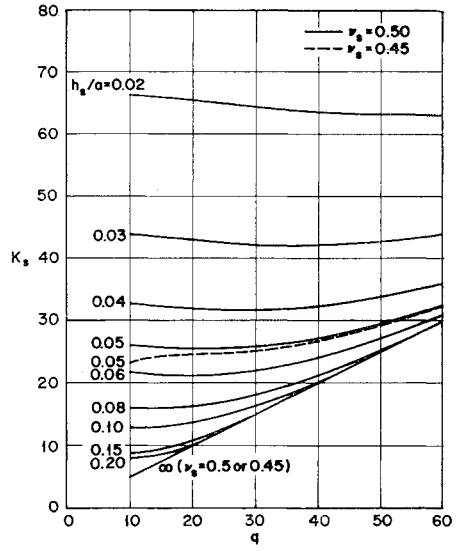

Fig. 7 Cushion stiffness coefficient.

at midlength and then rotated 180° and tested a second time. A fifth test was conducted, but the buckling pressures based on visual observation and on back-to-back strain-gage data were in marked disagreement, 27 and 40 psi, respectively, and the test point is not shown in Fig. 9. The motor cases were supported in saddles at the end bulkheads, and the midlength load was applied through a massive wooden chock lined with a 1.6-in.-thick rubber-like cushion. The same cushion was used for all of the tests. For purposes of expressing the experimental buckling load in terms of buckling pressure for the test points in Fig. 9, the pressure was assumed to have a simple cosine distribution over the top half of the cylinder circumference. Then

$$p_{exp} = (2/\pi ab)P_{exp} \tag{22}$$

where P_{exp} is the experimental buckling load. The stiffness characteristics of the cushion used in the tests apparently were not recorded. Data for supposedly similar cushions, furnished to the authors in private communication, indicate a nonlinear pressure-compression relationship with a tangent modulus of about 420 psi at the experimental buckling pressure. This value was used in plotting the test data in Fig. 9. The agreement between the theoretical and experimental buckling pressures shown in Fig. 9 is rather close. In all of the tests, the shell buckled into the series of localized circumferential waves, which is characteristic of buckling under a circumferential band of pressure, e.g., Fig. 5 of Ref. 2. The measured, circumferential buckle-wave length varied from about 7 to 8 in. The corresponding value given by the present theoretical analysis is 7.4 in.

Figure 9 also serves to illustrate the practical importance of cushion stabilization. The buckling pressure for a cushion stiffness of 420 psi is seen to be about four times as great as the corresponding value for fluid-pressure loading ($E_s = 0$). Although no experimental data are given in Fig. 9 for the fluid-pressure case, the agreement between present theory and corresponding experimental values for fluid-pressure loading is indicated in Fig. 10. These test data are from a report by

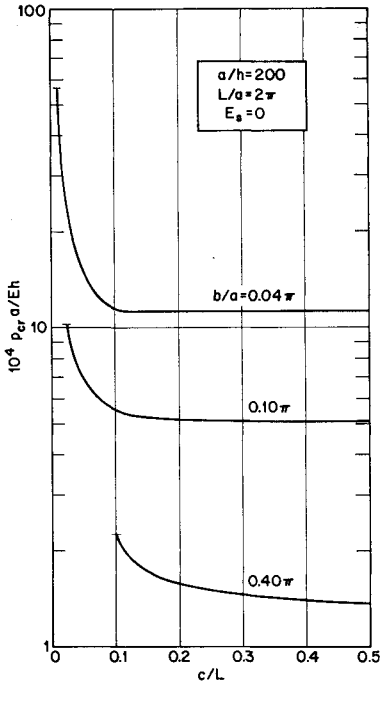

Fig. 6 Influence of pressure-band location.

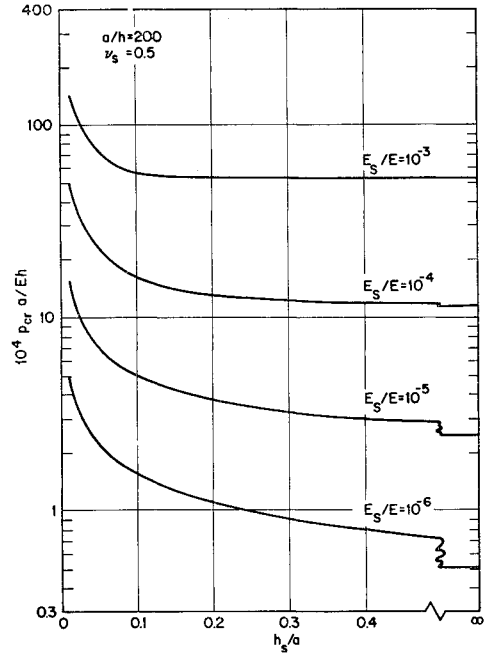

Fig. 8 Influence of cushion thickness for rings.

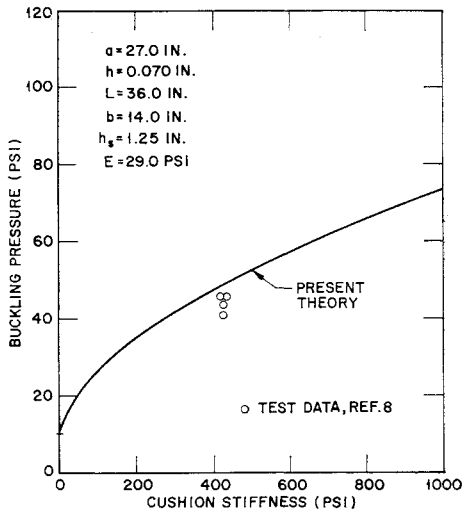

Fig. 9 Motor case buckling tests.

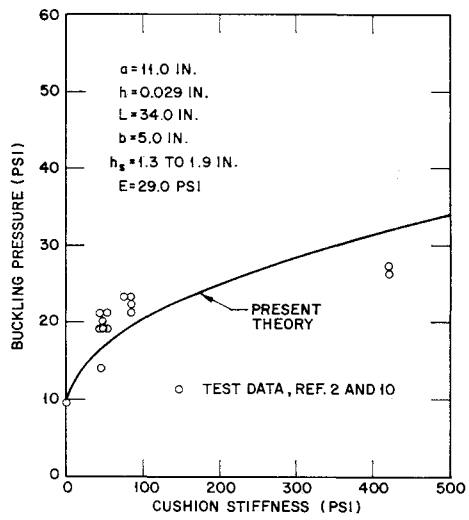

Fig. 11 Model-size cylinder buckling tests.

Goree and Nash.[9] The test pressure was axisymmetric and was applied through a constrained pneumatic tube encircling the test cylinder. The pressure-band width in those tests was only a small fraction of the cylinder length, as indicated in the figure.

The test data shown in Fig. 11 were obtained from tests of six 22-in.-diam steel cylinders. The test point for zero cushion stiffness is taken from Ref. 2. Loading in that test was axisymmetric and was applied through a constrained pneumatic tube which encircled the test cylinder at mid-length. The remaining test points are from Ref. 10 and represent transverse loading tests. In those tests, the cylinders were supported in saddles at the end bulkheads and loaded at mid-length through a heavy aluminum half-ring lined with a 2-in.-thick polyurethane cushion. Each cylinder was loaded to buckling three times, with the specimen rotated 90° between tests. Six cushions of different stiffnesses were used for the 13 test points shown. The stiffness characteristics of each cushion were determined from compression tests of segments cut from the cushion. The tests revealed that the mechanical properties were not entirely uniform throughout each cushion. Furthermore the pressure-compression plots were somewhat nonlinear in the pertinent compression range. The test cushion stiffness values shown in the graph represent average tangent-modulus values corresponding to the pressure at buckling in each case and can be considered to be only approximately correct. Equation (22) again was used to express experimental buckling load in terms of buckling pressure. The reported buckling loads were based on visual observation of the formation of buckle waves. Most of the cylinders were instrumented with back-to-back strain gages, which indicated characteristic strain reversal at the visually observed buckling load. In most cases the strain reversal at buckling was quite sharp. Two additional tests in which there was no visual criterion for buckling were reported for the stiffest cushion. In one of these the cylinder was instrumented with back-to-back strain gages, and these indicated strain reversal at an applied pressure of about 26 psi, a value in agreement with corresponding data in Fig. 11. The circumferential buckle-wave lengths for the tests with cushions in the 50 to 90 psi stiffness range were about 6 to 7 in. The corresponding theoretical values are about 5 to 6 in.

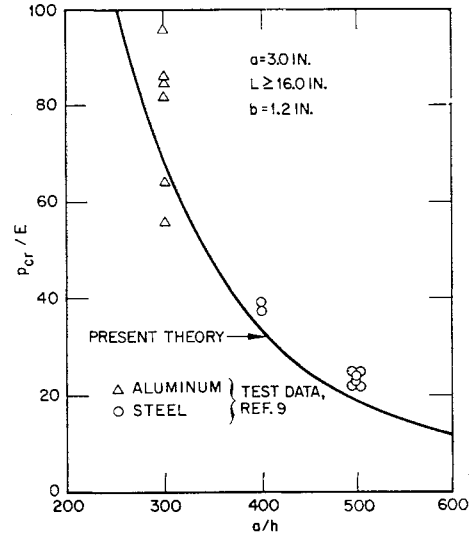

Fig. 10 Buckling under a band of fluid pressure.

Appendix: Cushion Stiffness Analysis

An approximate equation expressing the incremental pressure p_1 in terms of the displacement w_1 is readily obtained from an elastic analysis of the cushion. As noted, the cushion is assumed to be a linearly elastic, plane stress medium. The general solution of the two-dimensional problem in polar coordinates is given in Eq. (81) of Ref. 11. For plane stress, the solution yields the following expressions for the incremental stresses and displacements:

$$\left.\begin{aligned}
\sigma_r/E_s &= [-q(q-1)c_1r^{q-2} - q(q+1)c_2r^{-q-2} - \\
&\quad (q+1)(q-2)c_3r^q - (q-1)(q+2)c_4r^{-q}]\cos q\varphi \\
\tau_{r\varphi}/E_s &= [q(q-1)c_1r^{q-2} - q(q+1)c_2r^{-q-2} + \\
&\quad q(q+1)c_3r^q - q(q-1)c_4r^{-q}]\sin q\varphi \\
v_{s1} &= \{(1+\nu_s)q(c_1qr^{q-1} + c_2r^{-q-1}) + [(1+\nu_s)q + \\
&\quad 4]c_3r^{q+1} + [(1+\nu_s)q - 4]c_4r^{-q+1}\}\sin q\varphi \\
w_{s1} &= \{(1+\nu_s)q(c_1r^{q-1} - c_2r^{-q-1}) + [q(1+\nu_s) - \\
&\quad 2(1-\nu_s)]c_3r^{q+1} + [q(1+\nu_s) + 2(1- \\
&\quad \nu_s)]c_4r^{-q+1}\}\cos q\varphi
\end{aligned}\right\} \quad \text{(A1)}$$

where r is the (dimensional) radial coordinate, and q is an integer greater than unity.

Since the outer perimeter of the cushion is held fixed during the virtual deformation, and $a + h/2 \approx a$, the boundary conditions are

$$\left.\begin{aligned}
&\text{at } r = a + h_s: \qquad v_{s1} = w_{s1} = 0 \\
&\text{at } r = a: \qquad w_{s1} = w_1,\ \tau_{r\varphi} = 0
\end{aligned}\right\} \quad \text{(A2)}$$

These equations, together with the observation that $\sigma_r = p_1$ at $r = a$, determine the following relationship between p_1 and w_1:

$$p_1 = -K_s E_s w_1 \tag{A3}$$

where

$$K_s = N/\Delta$$

$$N = -2\frac{q^2-1}{q}\left\{\frac{3-\nu_s}{1+\nu_s}\lambda^{-2q} + q^2\lambda^{-2} - 2(q^2-1) + q^2\left[1 + \frac{8(1-\nu_s)}{(1+\nu_s)^2q^2}\right]\lambda^2 + \frac{3-\nu_s}{1+\nu_s}\lambda^{2q}\right\}$$

$$\Delta = 2\left\{(2q-1+\nu_s)\frac{3-\nu_s}{(1+\nu_s)q}\lambda^{-2q} - q(3-\nu_s)\lambda^{-2} + 2(1-\nu_s)\frac{q^2-1}{q} + (1+\nu_s)\,q\left[1 + \frac{8(1-\nu_s)}{(1+\nu_s)^2q^2}\right]\lambda^2 - (2q+1-\nu_s)\frac{3-\nu_s}{(1+\nu_s)q}\lambda^{2q}\right\} \tag{A4}$$

and $\lambda = 1 + (h_s/a)$.

The cushion stiffness coefficient K_s in Eq. (A4) is a function of the three parameters h_s/a, q, and ν_s. For $\nu_s = 0.5$, a graph giving K_s in terms of h_s/a and q is shown in Fig. 7. Selected values for $\nu_s = 0.45$ also are shown for comparison; the difference is seen to be small.

Two limiting cases may be noted. As the cushion thickness approaches infinity ($\lambda \to \infty$), Eq. (A4) reduces to $K_s = (q^2-1)/(2q+1-\nu_s)$. Second, as the cushion thickness goes to zero ($\lambda = 1.0$), $K_s \to \infty$. The latter result reflects the fact that the outer surface of the cushion is held fixed in a circular cylindrical configuration during the virtual deformation.

The expression for the cushion stiffness coefficient in Eq. (A4) and the graph in Fig. 7 are based on the conservative assumption that the cushion acts as a plane stress medium during the virtual deformation. The corresponding equations for plane strain may be obtained in the usual manner by replacing E_s and ν_s by $E_s'/(1-\nu_s'^2)$ and $\nu_s'/(1-\nu_s')$, respectively, in Eqs. (A3) and (A4).

References

[1] Brush, D. O. and Almroth, B. O., "Buckling of core-stabilized cylinders under axisymmetric external loads," J. Aerospace Sci. **29**, 1164–1170 (1962).

[2] Almroth, B. O. and Brush, D. O., "Buckling of a finite-length cylindrical shell under a circumferential band of pressure," J. Aerospace Sci. **28**, 573–579 (1961).

[3] Sanders, J. L., "Nonlinear theories for thin shells," Quart. Appl. Math. **21**, 21–36 (1963).

[4] Bodner, S. R., "On the conservativeness of various distributed-force systems," J. Aeronaut. Sci. **25**, 132–133 (1958).

[5] Langhaar, H. L., *Energy Methods in Applied Mechanics* (John Wiley and Sons, Inc., New York, 1962), p. 211.

[6] Lo, H., Bogdanoff, J. L., Goldberg, J. E., and Crawford, R. F., "A buckling problem of a circular ring," *Proceedings of the Fourth United States National Congress on Applied Mechanics*, (American Societies of Mechanical Engineers, New York, 1962), pp. 691–695.

[7] Almroth, B. O., "Buckling of a cylindrical shell subjected to nonuniform external pressure," J. Appl. Mech. **29**, 675–682 (1962).

[8] Miknis, A. C., "Simulated motor cases: buckling tests under lateral loading," Lockheed Missiles and Space Co., Rept. LMSD-800536 (April 1961).

[9] Goree, W. S. and Nash, W. A., "Elastic stability of circular cylindrical shells stabilized by a soft elastic core," Exptl. Mech. **2**, 142–149 (1962).

[10] Brush, D. O. and Morton, F. G., "Response of thin walled cylindrical shells to saddle-type loads," *Stress and Stability Analysis of Cylindrical and Conical Shells: Final Report, Vol. IV*, Lockheed Missiles and Space Co., Rept. LMSD-894808 (May 1961).

[11] Timoshenko, S. and Goodier, J. N., *Theory of Elasticity* (McGraw-Hill Book Co., Inc., New York, 1951), 2nd ed., p. 116.